IOPscience iopscience.iop.org

Home Search Collections Journals About Contact us My IOPscience

Nanoferroelectrics: statics and dynamics

This article has been downloaded from IOPscience. Please scroll down to see the full text article.

2006 J. Phys.: Condens. Matter 18 R361

(http://iopscience.iop.org/0953-8984/18/17/R02)

View the table of contents for this issue, or go to the journal homepage for more

Download details:
IP Address: 129.252.86.83
The article was downloaded on 28/05/2010 at 10:22

Please note that terms and conditions apply.

INSTITUTE OF PHYSICS PUBLISHING JOURNAL OF PHYSICS: CONDENSED MATTER

J. Phys.: Condens. Matter **18** (2006) R361–R386 doi:10.1088/0953-8984/18/17/R02

TOPICAL REVIEW

Nanoferroelectrics: statics and dynamics

J F Scott

Earth Sciences Department, University of Cambridge, Cambridge, UK

Received 18 January 2006, in final form 8 March 2006
Published 13 April 2006
Online at stacks.iop.org/JPhysCM/18/R361

Abstract
A topical review is given of the physics of submicron ferroelectrics, describing the application considerations for memory devices (both as switching memory elements for ferroelectric nonvolatile random access memories, FRAMs, and as passive capacitors for volatile dynamic random access memories, DRAMs) as well as the fundamental physics questions regarding both the thickness and lateral size of present interest.

(Some figures in this article are in colour only in the electronic version)

Contents

1. Introduction: scaling of parameters with size 362
 1.1. Relaxation thickness 363
 1.2. Confinement energies 364
2. Device applications 364
 2.1. The ultimate memory 364
 2.2. Three-dimensional capacitors 365
 2.3. Nanotubes and applications to microfluidics 365
 2.4. Self-assembly 367
3. Theory—ab initio models 368
4. Statics 368
 4.1. Geometric relations 369
 4.2. Focused ion-beam technology (FIB) and ultra-thin single crystals 369
 4.3. (3D) trenching and ferroelectric sidewalls 371
5. Dynamics 372
 5.1. Minimum switching time 372
 5.2. Rate-limiting switching mechanisms 372
 5.3. Skyrmions 373
 5.4. Ionic space-charge-limited current transients 376
6. Conduction mechanisms 377
 6.1. Schottky and Simmons 377
 6.2. Poole–Frenkel mechanism 379
 6.3. Fowler–Nordheim tunnelling 379

0953-8984/06/170361+26$30.00 © 2006 IOP Publishing Ltd Printed in the UK

6.4. Breakdown 379
7. Tunnel junctions 380
8. Polyvinylidene difluoride (PVDF) 381
9. Circular and toroidal ordering 381
10. Magnetoelectrics (multiferroics) 381
11. The future 383
Acknowledgment 383
References 383

1. Introduction: scaling of parameters with size

The fact that certain static and dynamic properties of ferroelectrics and ferromagnets scale with size has been known for more than 40 years. In 1946, Kittel derived the square root relationship between the magnetic domain stripe width w and film thickness d

$$w^2/d = \text{constant}, \tag{1a}$$

a formula that has been independently rederived for ferroelectrics by numerous authors, including Mitsui and Furuichi (1953) and Roytburd (1976). Here the constant is not arbitrary but given originally as

$$w = 0.54[\gamma d(\varepsilon_a \varepsilon_b)^{1/2}/P_0]^{1/2}, \tag{1b}$$

and by similar equations in more recent models. Here γ is the domain wall energy; ε_i, dielectric constants; and P_0, polarization far below T_c. $\gamma(PbTiO_3)$ is 10× larger than $\gamma(BaTiO_3)$, but $(\varepsilon_a \varepsilon_b)^{1/2}$ is 10× smaller; so $w(d)$ is nearly the same in these materials.

Using the later work of Zhirnov (1958, 1959), who showed that the domain wall thickness δ is rather constant over most ranges of d, we can rewrite equation (1) as

$$w^2/\delta d = G \tag{2}$$

where G is a geometric constant (see the diagram in figure 1). Equation (2) is an expression apparently without previous publication. It has the attractive quality that the constant G is dimensionless. It depends upon strain and elastic coefficients such as C_{11} and basically relates surface energy to domain wall energies. For $BaTiO_3$ or $PbTiO_3$ the constant is about 36 (and the wall thickness $\delta = 1$ nm) and it fits data, as shown in figure 2, from a few nanometres (Streiffer *et al* 2002) to hundreds of nanometres (Schilling *et al* 2006), to millimetres (Mitsui and Furuichi 1953). For Rochelle salt, the constant G is very nearly unity (Zhirnov 1958, 1959) (and the wall thickness δ is about 12 nm), which is accidental but charming.

It is interesting that this relationship among static geometric parameters fits experimental data over six decades of specimen thickness d; we find in addition that dynamical parameters also scale with thickness: the law of Kay and Dunn (1962) for coercive field $E_c(d)$ satisfies

$$E_c(d) = gd^{-2/3} \tag{3}$$

for about six decades of thickness as well (here g is a d-independent constant), using combined data for several ferroelectrics (Dawber *et al* 2003, 2005). The Kay–Dunn law was originally derived under assumptions of homogeneous nucleation and very large activation energies—hypotheses that even its authors found explicitly unphysical. However, recently Chandra *et al* (2004) rederived the Kay–Dunn law under realistic assumptions of inhomogeneous nucleation, which is generally the situation in almost all real ferroelectrics at low to moderate fields. Equation (3) is compared with experimental data in figure 2, together with equation (2). The results show that both dynamic switching properties such as coercive field and static properties such as domain stripe width scale with thickness in a way we understand from millimetre

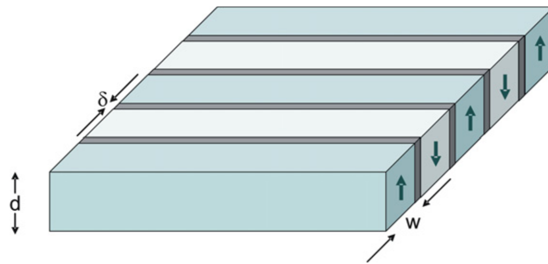

Figure 1. Diagram of domain stripe geometry: d is crystal thickness; w, 180° domain stripe width; δ, domain wall thickness.

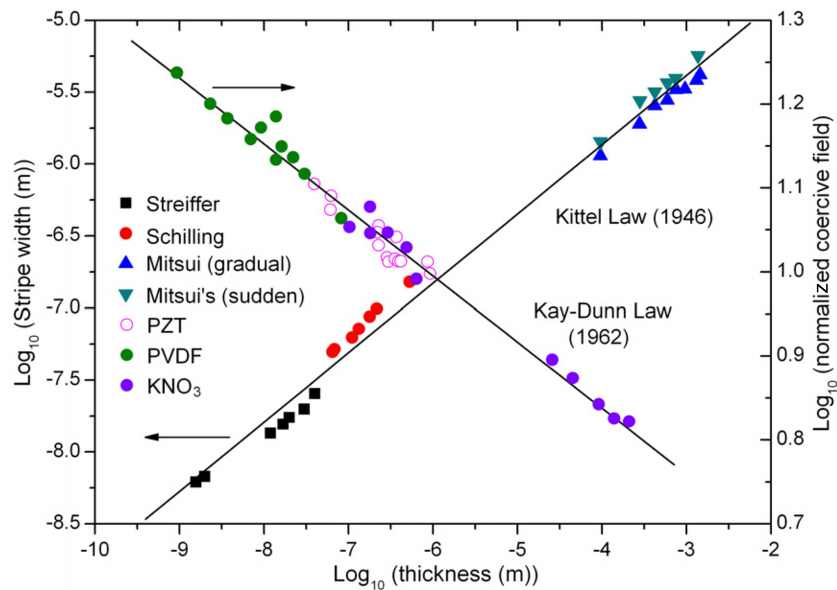

Figure 2. Graph of 180° domain stripe width $w(d)$ and coercive field $E_c(d)$ versus film thickness d for several ferroelectrics. This log–log scale shows that $E_c = ad^{-2/3}$ (Kay–Dunn law) and $w = bd^{1/2}$ (Kittel law) from about 1.5 nm to 1.5 mm—six decades of thickness. Taken from Dawber *et al* (2003) and Schilling *et al* (2006).

thickness down to nanometre thickness. When the Fermi–Thomas screening in the metal electrodes is carefully included (Dawber *et al* 2003), the scaling continues down to about 2.4 nm, at which point the ferroelectricity becomes unstable, both experimentally (Tybell *et al* 2002) and theoretically (Junquera and Ghosez 2003). It is not certain yet whether this instability in a single-domain ground state results in paraelectricity or in many small domains.

1.1. Relaxation thickness

Rather careful studies of polarization have been made in a series of ferroelectric films from 4 to 20 nm thickness. Following Tybell *et al* (1999) who went down to 4 nm, or Yanase *et al* (1999), who reached 12 nm, more detailed results were presented by Nagarajan *et al* (2004) and Prasertchoung *et al* (2004), who studied PZT films down to 4 nm, measuring both the c/a tetragonality and the polarization dependence on film thickness, and making quantitative

comparisons with the theories of Junquera and Ghosez (2003) and of Glinchuk *et al* (2002). However, as discussed below, based on the ultra-thin single-crystal studies of Saad *et al* (2004), it now appears that the shifts in Curie temperature and other parameters as functions of film thickness are usually not intrinsic, and so detailed quantitative comparisons with the theories of Kretschmer and Binder (1979) or of Li *et al* (1996, 1997), or Glinchuk and co-workers may be moot or at best premature. For films less than $d = 20$ nm thick, the c/a ratio increases about 1% from the bulk value; for $d > 20$ nm this excess tetragonality relaxes via dislocation formation. 15–20 nm appears to be the characteristic length above which relaxation sets in. Down to $d = 15$ nm there is no significant decrease in spontaneous polarization from the bulk values; below this thickness the films are too leaky for quantitative tests.

1.2. Confinement energies

Although several papers have been published reporting confinement energies as large as 1 eV in ferroelectrics with submicron lateral widths (Yu *et al* 1997, Kohiki *et al* 2000), my view (Scott 2000b) is that these are all artefacts. Measurable confinement energies require electron mean-free paths λ that are much greater the lateral dimensions. In turn, this requires high-mobility samples at low temperatures. The existing experiments are on low-mobility semi-insulating ceramics at room temperature. Interpretations of these data as ferroelectric quantum dots with confinement energies are therefore not credible. In the case of strontium bismuth oxide (SBT), the report (Kohiki *et al* 2000) of a band gap much lower than the bulk SBT value (Hartmann *et al* 1999) of 4.0 eV is probably due to a thin surface layer of bismuth oxide Bi_2O_3 that has phase separated and is known (Zhou *et al* 1992) to have that band gap energy. Phase separation of Bi is well established in these materials (Watts *et al* 2004).

2. Device applications

Although fundamental questions of the minimum size for ferroelectricity are of significant academic importance, in order for this topic to be of wider interest, there must be a technological need driving it. In this case it is the need for smaller, faster, lighter, high-density (many Gbit) computer memories. The most pressing embodiment is for the next generation of hand-held telephones, which must be able to interface with the internet and download large files and photographs, both still and video, plus high-quality audio. The present review does not do justice to the extensive device development in Japan; led by Professor Ishiwara's group at Tokyo Institute of Technology (Funakubo and co-workers), they have produced bismuth titanate FRAMs of $d = 13$ nm thickness with an impressively low 0.5 V saturation, as well as strontium bismuth tantalate (SBT on HfO_2) memories with ferroelectric gates and non-destructive read-out (5 μm gate lengths and >16 day retention) (Ishiwara *et al* 2004). Similar progress has been made by Kim and co-workers in Korea (Yoon *et al* 2006). A particularly good review of thin-film devices emphasizing interfacial physics has just appeared by Auciello (2006).

2.1. The ultimate memory

Table 1 from IMEC (Wouters 2006) lists the properties desired for the ultimate memory (UM), which we might hope to approximate in the next generation of computer memory devices. The ferroelectric random access memory (FRAM) is one of the strong candidates for realization of such a memory.

Table 1. Required parameters for the ultimate memory of the (near) future. Wouters (2006), IMEC (ISIF, Shanghai, April 2005; unpublished).

Specification	Ultimate memory target
Memory size	16–64 Mb
Cell size	<15 F^2
Area scalability	45 nm technology and below
Process complexity	<5–6 extra masks
Read access speed	$t_{acc} < 10$ ns
Write voltage	$<V_{dd}$
Write current	$<50\ \mu$A
Read current	15 μA
Write addressability	Bytewise, NO refresh
Read endurance	$>10^{15}$ (unlimited)
Write endurance	$>10^{12}$
Retention	10 years
Temperature window	−40–85 °C (150 °C automotive)

Table 2. International Technology Roadmap for Semiconductors requirements for FRAM development (http://public.itrs.net/Files/2002Update/Home.pdf).

Year of production	2004	2005	2006	2007
FRAM technology node—F (nm)	220	180	150	130
FRAM cell size—area factor a in multiples of F^2	16	10	10	10
FRAM cell size (μm^2)	0.518	0.324	0.225	0.169
FRAM cell structure	1T1C	1T1C	1T1C	1T1C
FRAM capacitor structure	Stack	Stack	Stack	3D
Ferro capacitor voltage (V)	1.8	1.5	1.3	1.2
FRAM endurance (read/write cycles)	1.00×10^{15}	$>1 \times 10^{16}$	$>1 \times 10^{16}$	$>1 \times 10^{16}$
FRAM non-volatile data retention (years)	10	10	10	10

2.2. Three-dimensional capacitors

Table 2 from the International Technology Roadmap for Semiconductors shows that size limitations dictate that by next year (2007), three-dimensional integration of capacitors will be required to achieve competitive multi-Gbit FRAM densities. The existing stacked planar devices will be inadequate. This can be done in a variety of ways, such as bending over the top electrode and dielectric, as shown in figure 3 from IMEC (Menou *et al* 2005, Goux *et al* 2005), or via coating a high aspect ratio trench with a thin layer of dielectric, as done (Funakubo *et al* 2005) by a Samsung–Tokyo Institute of Technology collaboration (figure 4). The design used in figure 3 achieves a 50% increase in capacitance but had problems getting the strontium bismuth tantalate (SBT) all into the proper ferroelectric phase. The design used in figure 4 employs lead zirconate titanate (PZT) on Ru electrodes, but unlike that in figure 3 is not yet device-worthy as a commercial process. Figure 5 illustrates work from our Cambridge laboratory (Miyake *et al* 2006) with very good coverage of Ru electrodes.

2.3. Nanotubes and applications to microfluidics

Figure 6 illustrates an array of ferroelectric nanotubes from our laboratory. The present problem of achieving conformal step coverage of inner and outer concentric cylindrical electrodes has taken time to optimize. Initially we used Pd electrodes deposited via Pd-acetate.

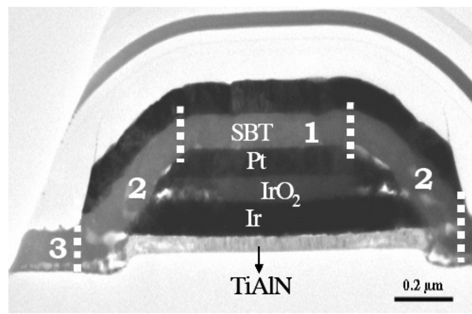

Figure 3. Scanning electron micrograph (SEM) cross-section of (3D) ferroelectric random access memory (FRAM) capacitor using strontium bismuth titanate (SBT) from the group of Wouters at IMEC (Menou *et al* 2005).

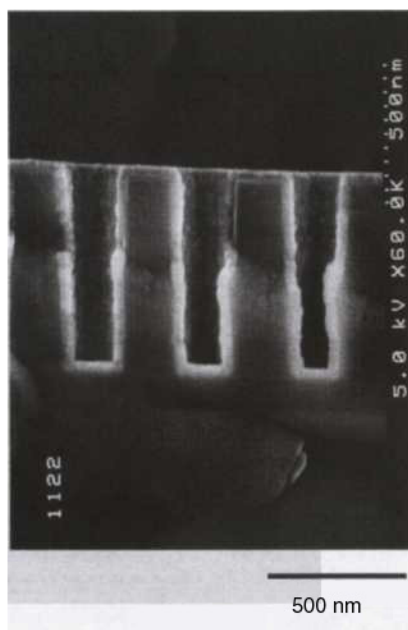

Figure 4. SEM cross section of Ru electrode coverage in a trenched capacitor structure for FRAMs on a silicon chip, using Ru-DER precursor and chemical vapour deposition (CVD) (Funakubo *et al* 2005).

However, this gave submicron granules that did not wet the ferroelectric nanotubes. More recently (figure 5) we had good results with Ru, deposited as organic Ru-DER ((2,4-dimethylpentadienyl)(ethylcylopentadienyl) ruthenium) (Miyake *et al* 2006).

The applications of such nanotubes are likely to include microfluidics (Kenis and Stroock 2006), such as drug delivery systems or ink jet printers. In the longer term, such high-dielectric nanotubes can be used for (3D) capacitors in random access memories. Some utilization for electrooptic or photonic arrays is also possible.

From a more academic point of view, misfit dislocations for ferroelectric nanotubes grown epitaxially onto substrates present interesting phase diagrams (Bobylev *et al* 2003, Gutkin *et al* 2000, 2001). For planar structures misfit dislocations are created freely to minimize strain

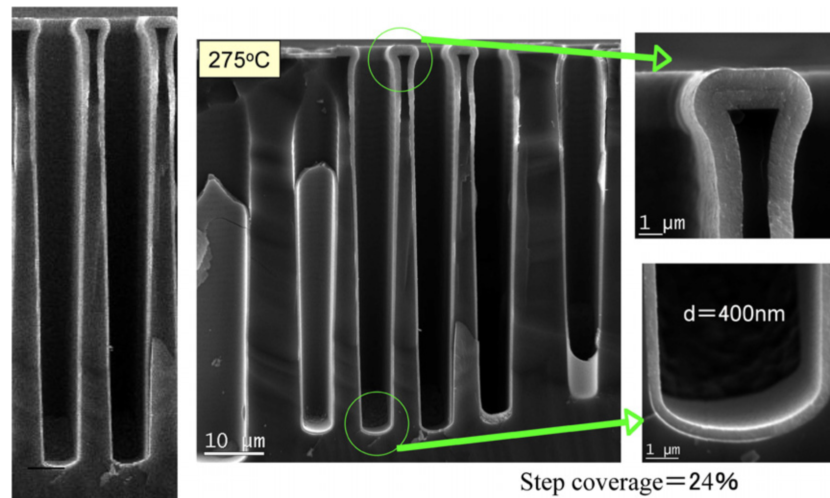

Figure 5. SEM cross section of Ru electrode coverage in a trenched capacitor structure for FRAMs on a silicon chip, using Ru-DER precursor and misted chemical solution deposition (CSD) (Miyake *et al* 2006).

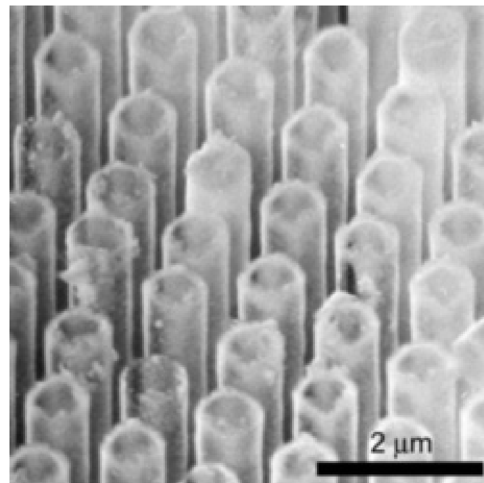

Figure 6. Ferroelectric nanotube array of strontium bismuth tantalate (SBT) (Morrison *et al* 2003).

caused by lattice mismatch. But the cylindrical boundary conditions of a nanotube make such misfits cost energy. The result is a rich phase diagram for phases with random sparse misfit dislocations, dense periodic misfits, or none at all when temperature is plotted versus substrate misfit parameter; for very small diameter nanotubes epitaxially on inner (or outer) substrate cores, misfit dislocations are energetically forbidden.

2.4. Self-assembly

The first self-assembling nanoferroelectrics were reported by Alexe *et al* (1998, 1999) and Scott *et al* (1998) for Bi_2O_3 phase separation from bismuth titanate films, forming a self-patterned

top electrode. The phase separation of Bi on surfaces of ferroelectrics has more recently been studied by Watts *et al* (2004). A detailed theory and experiment report modelling short-range correlations in position was given by Dawber *et al* (2003) for PZT islands, following the theory of Shchukin and Bimberg (1999) and Williams *et al* (2000). Nanoislands of ferroelectrics repel each other through a substrate-mediated strain first analysed by Andreev (1981). Some earlier work on ferroelectric islands includes that of Siefert *et al* (1996) who studied $PbTiO_3$ islands on (001) $SrTiO_3$ substrates; and later Roelofs *et al* (2002) examined similar ferroelectric nanodots, as did Shimizu's group (Nonomura *et al* 2003, Fujisawa *et al* 2004, Shimizu *et al* 2004) who obtained thicknesses as small as 1.7 nm and 38 nm lateral diameters. These self-assembling nanoferroelectrics generally exhibit only short-range ordering, but registered arrays can be fabricated by incorporating submicron, monodisperse latex spheres in the deposition (Ma *et al* 2003, Ma and Hesse 2004).

3. Theory—*ab initio* models

In contrast with these engineering priorities, the impetus for theoretical work is to interface with *ab initio* models. In the past decade these models have replaced the classical ball-and-stick model of ferroelectricity with a Berry phase formalism in which the electric polarization P is the quantum mechanical observable in a Stokes-theorem calculation. Although the size (number of atoms/ions) in these model calculations is now approaching that of experimental nanophase specimens, only in the past year have the calculations been for finite electric fields E (Wu *et al* 2005), and even those finite-E models are for $T = 0$ zero-temperature conditions. It will be necessary for many phenomena to carry out *ab initio* calculations in finite fields and temperatures, and for somewhat larger arrays of atoms/ions. The lateral nanoscale may also require abandonment of the circular (or cylindrical) boundary conditions often imposed, particularly for toroidal or circular ordering of domains in nanodots and nanowires. That is, paradoxically, the cylindrical boundary conditions used at present are limited by computer power, whereas the ones required for nanotubes have periods dictated by the actual circumference and are not arbitrary; the new cylindrical boundary conditions are real.

Prior to the development of *ab initio* models for this problem there were three or four phenomenological models based upon Landau theory that are worthy of note: the first papers emphasizing depolarization fields and the role of screening in the metal or semiconducting electrodes were in the USSR by Ivanchik (1961), Guro *et al* (1968, 1970), and Vul *et al* (1970), and in the USA by Batra *et al* (1973). This was followed by a detailed depolarization model of Tilley and Zeks (1984). More recently, two papers by Li *et al* (1996, 1997) include the anisotropy of the correlation functions in the problem and derive results in good agreement with experiment for lead titanate, as well as a correlation length of 2.4 nm that agrees exactly with that later determined by Dawber *et al* (2003) and Junquera and Ghosez (2003). Finally, Zhang *et al* (2001) combine finite size effects including depolarization and stress in a simple analytic model.

4. Statics

Before worrying about the effects nanosize dimensions have on dynamic properties such as coercive fields and switching times, it is useful to look at the static geometric properties of ultra-small systems. Because the surface-to-volume ratio is large in such specimens, parameters such as domain wall width w and wall thickness δ, which depend upon subtle ratios of domain wall energy to surface energy, can be remarkably different from bulk values. Parenthetically we

Figure 7. Focused-ion beam production of ultra-thin ($d = 70$ nm) single crystal ferroelectric (Saad *et al* 2004).

note that these results are very different for magnetic domains, where the exchange interaction is strong, and in ferroelectrics, where the coupling between local polarizations is weak. As a result ferroelectric domain walls are typically 1–10 nm in thickness, whereas in magnets they may be hundreds of times thicker.

4.1. Geometric relations

In extending the earlier work of Kittel (1946) to ferroelectrics, Mitsui and Furuichi (1953) derived explicit relationships between domain stripe widths w for 180° domains in barium titanate. As in the Kittel formula, they found $w = cd^{1/2}$, where c is a constant related to the surface energy of the system, and hence to the wall energy γ and the dielectric constants ε parallel and perpendicular to the polarization. Their experiments were limited to sample thicknesses d of order millimetre size. A few years later Zhirnov (1958, 1959) derived similar relationships for the domain wall thickness δ and showed that $\delta =$ about 1 nm in $BaTiO_3$ but 12 nm in Rochelle salt. In general it is not easy to measure separately and unambiguously the parameters that appear in the expressions for G in equation (1) from Zhirnov or Mitusui and Furuichi, but none is an adjustable parameter. The result is that the constant G will have some temperature dependence, but not vary strongly with T except in the case of T near a phase transition temperature (Yacoby 2006).

4.2. Focused ion-beam technology (FIB) and ultra-thin single crystals

FIB processing of ultra-thin single crystals and (3D) structures, originally by Ganpule *et al* (1999) and subsequently by Gregg and co-workers (figures 7 and 8) has been explored by several groups. Using this technique the group of Gregg, Bowman and co-workers at Queen's University, Belfast, have succeeded in making (figures 7–9) free-standing single crystals of both barium titanate and strontium titanate down to 60 nm thickness with no substrate misfit strain and identical top and bottom electrodes, from which it was determined (Saad *et al* 2004) that intrinsic electrostatic effects (depolarization fields) are unimportant at such thicknesses.

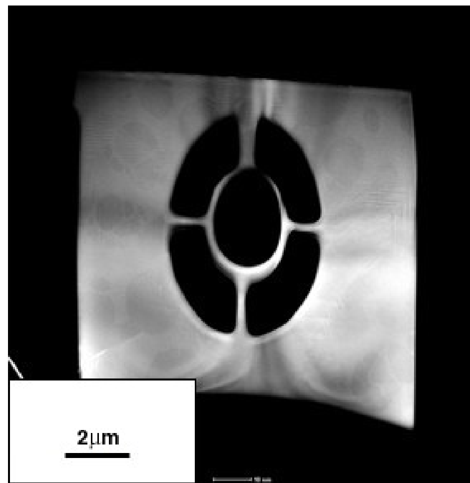

Figure 8. SEM micrograph of (3D) single-crystal ferroelectric structure produced via focused ion beam (Gregg *et al* 2006).

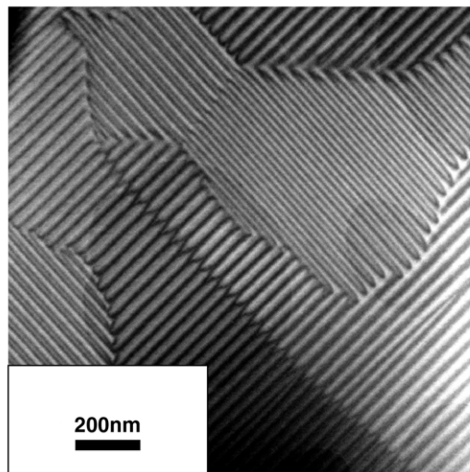

Figure 9. STEM micrograph of nanodomains in a $BaTiO_3$ FIB-cut single crystal of about 80 nm thickness (Gregg *et al* 2006).

This is compatible with the data shown in figure 2, but it contradicts the conventional wisdom for ferroelectric thin films. The prevailing wisdom had been that films thinner than $d = 1\ \mu$m had peaks in their dielectric constants $\varepsilon(T)$ that were severely broadened (hundreds of degrees wide) and significantly shifted in peak temperature (>100 K) from depolarization fields. The new work by Saad and co-workers shows, to the contrary, that these effects are extrinsic, probably caused by oxygen vacancy gradients in the ceramic films (Bratkovsky and Levanyuk 2005).

Note that although most commercial devices will employ fine-grained ceramic films, single crystals are not limited to academic interest; a high-density data storage system based upon scanning nonlinear dielectric spectroscopy was detailed by Cho *et al* (2002) using thin films of single-crystal ferroelectric lithium tantalate.

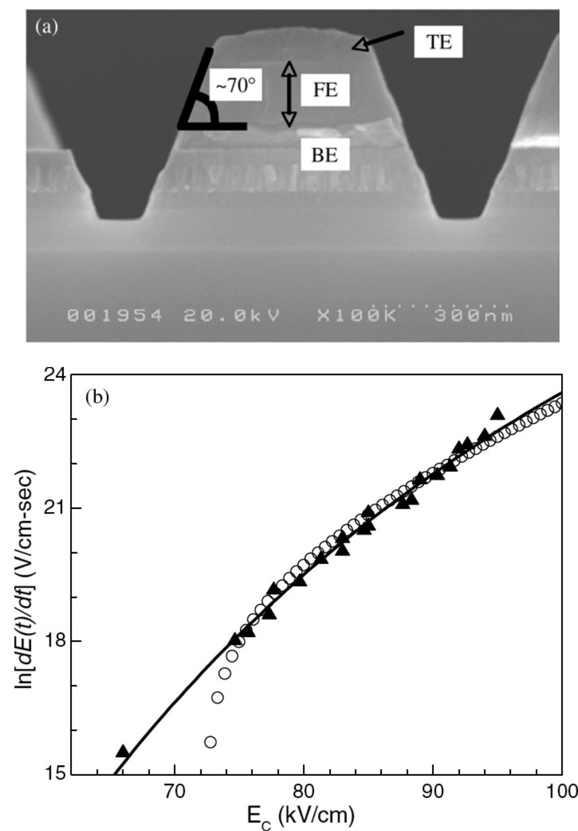

Figure 10. SEM cross section of 0.32 μm^2 PZT FRAM cells with truncated cone structure (a), and (b) ramp rate versus coercive field for 0.19 μm^2 PZT capacitors, showing agreement with the Pulvari nucleation-limited model and disagreement with the Landauer domain wall speed-limited model (Jung *et al* 2005).

4.3. (3D) trenching and ferroelectric sidewalls

The idea that one could readily increase the capacitance of a memory array by extending the capacitors down the sidewalls of three-dimensional trenches is not new. However, there are problems to overcome even within the electrostatics of such situations. Firstly, as shown in figure 10(a), the actual capacitors in state-of-the-art Samsung FRAMs are truncated cones. The fringing field effects for such geometries are large and not easily calculated from standard analytic models, such as that for cylinders (Jung *et al* 2005). However, estimates made from a simple equation due to Feynman give reasonable agreement with experiment: Feynman points out that one can estimate fringing field corrections ΔC to capacitance by pretending that the effective capacitor area A is not the real capacitor area w^2, but $(w + 3d/8)^2$, where w is the lateral width (about 450 nm in Jung's case) and the thickness $d = 144$ nm. This gives an effective area of approximately $A' = w^2 + 3dw/4 + 9d^2/64$, whence $\Delta C = 3dw/4 + 9d^2/64$. When graphed versus thickness d, ΔC will average the linear and quadratic terms in d (since w and d are comparable) to a constant times d^n, where $n =$ about 1.5. Jung found empirically that the fringing field correction ΔC varied approximately as $d^{1.6\pm0.1}$. Such fringing fields will be important for nanocapacitors, especially as the aspect ratios change with attempts to make deeper trenches and nanotubes.

5. Dynamics

One of the interests for both fundamental physics and device applications is the minimum switching time for a ferroelectric. This is paramount in engineering chip design for FRAMs, although at present the access times of 60–100 ns are determined by other factors, such as 5 V operating logic levels and integrated displacement charge required for sense amplifier margins. From a fundamental point of view, understanding the minimum switching time necessitates identification and minimization of the rate-limiting parameter.

5.1. Minimum switching time

A few years ago the author (Scott 2000a) estimated this as $t_s = 600 \pm 100$ ps in the asymptotic high-voltage limit. This estimate was based on nucleation rates R extracted independently from switching current transient lineshapes $I(t)$, where I is the displacement current in a non-conducting sample. This estimate follows from Duiker's model

$$t_s = (1/v)[(vD/Rk)^{1/(D+1)} - r_c], \tag{4a}$$

where v is the domain wall speed; D, the dimensionality of domain growth; R, a nucleation rate that can be measured independently from the current transient pulse shape $I(t)$; k, a numerical constant $= 4\pi/3$ for $D = 3$; and r_c, the minimum radius of a nucleating domain, above which domains grow rather than shrink (about 1 nm). If we neglect r_c (and thereby necessarily overestimate t_s) and set v equal to the speed of sound v_s (supersonic domains have never been observed directly in ferroelectrics), we find from equation (4*a*) that

$$t_s \leqslant v_s^{3/4}(9R/4\pi) = 600 \pm 100 \text{ ps}. \tag{4b}$$

Very recently, however, a faster switching of 280 ps was measured experimentally (Li *et al* 2004). This has reopened the question and indeed suggests that, although the theory necessarily gives an overestimate of switching time, the experimental result is faster by a factor of two and outside the estimated uncertainties; therefore there might be additional unexpected processes that make the sub-nanosecond speed even faster than earlier theoretical estimates based upon inhomogeneous nucleation. We consider that possibility—additional nucleation at high fields—below in section 5.3.

5.2. Rate-limiting switching mechanisms

Because ferroelectric domain switching usually initiates itself at defect sites, particularly at the electrode/dielectric interface, the nucleation is inhomogeneous. Depending upon conditions, the rate-limiting step in switching can be the nucleation time or the speed of domain walls after they are nucleated. Both situations are well known: in bulk under moderate fields, switching in perovskite oxides such as $BaTiO_3$ is limited by (sideways) domain wall speeds; in water-solution-grown ferroelectrics such as TGS (triglycine sulfate) or GASH (gadolinium aluminium sulfate hexahydrate), it is nucleation limited. However, if we consider nanoferroelectrics, there will always be a lateral size below which the process is nucleation limited. (This is simply because for small enough specimens the number of nucleation sites will be a handful (3 or 2 or 1 . . . or zero).) For KNO_3 Scott *et al* (1986) estimated this lateral area as 100 μm^2; for PZT, he estimated 1 μm^2. Recent studies (Jung *et al* 2002, 2005) comparing coercive fields $E_c(f)$ versus frequency for KNO_3, barium strontium titanate (BST), PZT, and strontium bismuth tantalate (SBT) strongly support the nucleation-limited model. Further support is provided by examining the dependence of E_c upon ramp rates dE/dt of applied fields compared with the theories of Landauer *et al* (1956), which neglected nucleation, and of Pulvari and Kuebler

(1958), which included it; these verify the estimate of critical lateral area of about 1 μm^2 by examining PZT capacitor areas of 0.19, 0.32, and 166.0 μm^2. Figure 10(b) shows that the Pulvari–Kuebler model, with nucleation, fits the 0.19 μm^2 data much better than does the Landauer model, which neglected nucleation.

5.2.1. Ishibashi–Avrami domain wall speed limited. Ishibashi's model (Ishibashi and Takagi 1971) assumes that the rate-limiting parameter in ferroelectric switching is the domain wall speed (a combination of forward growth and sideways growth). It is based upon the earlier model of Avrami for crystallization. In order to make the mathematics analytically tractable, Ishibashi assumes that the domain wall speed v is independent of domain radius; in reality this is a bad approximation, since v varies approximately as $1/r$. The result is that the model describes switching well in terms of its functional dependence upon applied field E and dimensionality of domains D, but some of the fitting parameters are inaccurate numerically. Averaging forward growth (needle-like) and sideways growth results in a dimensionality that can be non-integer, but this is not a real Hausdorf fractal dimension. Similarly, neglecting the $1/r$ dependence of v will also yield slightly unphysical non-integer dimensionality. Nevertheless, this model proved to be a substantial improvement over earlier models, which typically had the same or larger numbers of fitting parameters. Two cases were separately considered, one of which had pre-existing nanodomains embedded as seeds for switching.

5.2.2. Du–Chen nucleation limited. In contrast to the Ishibashi–Avrami model above, Du and Chen (1997, 1998) developed a model in which nucleation is the rate-limiting parameter in switching. Jung *et al* (2002) were able to show that the Du–Chen model was superior to that of Ishibashi in modelling the high-frequency dependence for several thin-film (about 120–300 nm) ferroelectrics (potassium nitrate, KNO_3; barium strontium titanate, BST; strontium bismuth tantalate, SBT; and lead zirconate, PZT) in large lateral sizes, and Jung *et al* (2005) later showed further that the switching-speed limitation from nucleation became noticeable at all frequencies for submicron diameter capacitors of PZT (width about 450 nm).

A similar nucleation-limited model was published by Tagantsev *et al* (2002) without reference to the original 1998 work of Du and Chen.

5.3. Skyrmions

Gruverman (1989) and Shur *et al* (1990, 1991) discovered that in lead germanate ($Pb_5Ge_3O_{11}$), where 180° domains are optically distinct due to electro-gyration, at high applied electric fields E (>150 kV cm^{-1}) there is a threshold above which the domain wall suddenly thickens. Under higher resolution it may seen that the domain wall is rather frothy, and nanodomains are nucleated in front of the advancing macroscopic domain wall (figure 11). We interpret these anomalies as skyrmions, which are chiral topological defects. These produce nucleation of nanodomains through a wall-roughening process (Rice *et al* 1981). A very similar effect was reported in ferromagnets by Randoshkin (1995a, 1995b) in a single-crystal film of iron garnet (figure 12), where the domain walls also appear foamy above a critical applied field. It is important to note in both figures 11 and 12 that the macroscopic domain wall surface becomes wavy just below the nanodomain emission threshold; the walls at lower fields and velocities are quite flat. Therefore the nanodomain ejection from the wall has a precursor in the domain wall curvature. In magnets the phenomenon is modelled via a spin-wave formalism based upon the gyrotropic model of domain wall motion in uniaxial materials. When an applied magnetic field is sufficiently strong to exceed the Walker threshold, the magnetization vectors in the domain wall begin to precess around the applied field H with frequency $\omega = \gamma H$, where γ is the

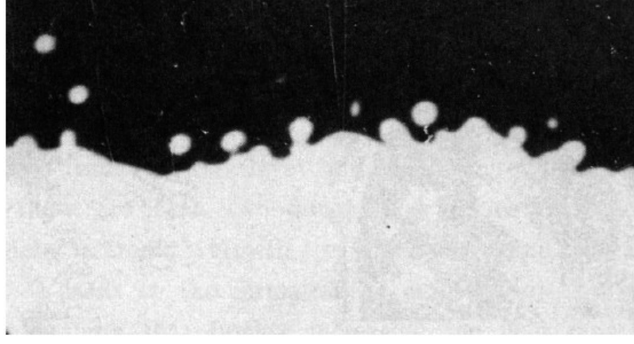

Figure 11. Optical micrograph of nanodomains created in lead germanate in front of a large advancing domain wall (Gruverman 1989).

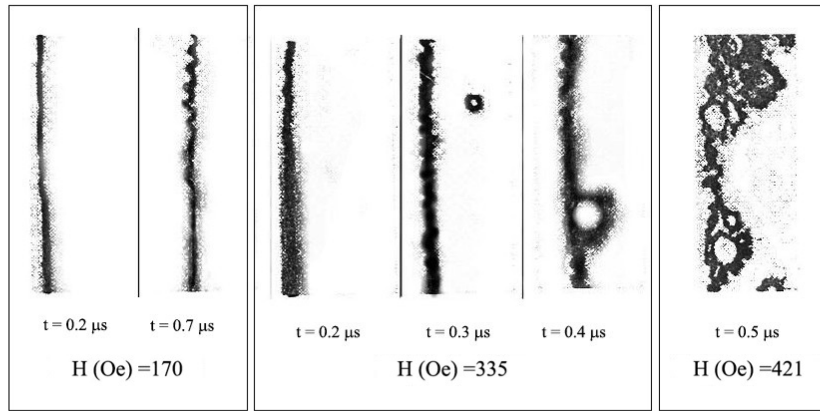

Figure 12. Micrograph of magnetic nanodomains ejecting from inside a large domain in iron garnet (Randoshkin 1995a, 1995b).

effective gyromagnetic ratio. We note that the domains nucleated in front of the large domain wall may be regarded as vortex-like skyrmions. The suggestion that follows then is that the domain wall phenomena in lead germanate might also be described by a gyrotropic model.

The model of Kudryavtsev *et al* (1998).

The (2D) Langrangian developed by these authors is of the form

$$L = F[(1/2)\partial_\alpha\phi\partial^\alpha\phi - (k^2/4)(\partial_\alpha\phi x\partial_\beta\phi)(\partial^\alpha\phi x\partial^\beta\phi) - (\mu^2/2)(1-\phi_3^2)] \quad (5)$$

(where y is along the domain wall and x normal to the wall) and results in small amplitude waves propagating along the wall (the waviness also shown in figures 11 and 12) of amplitude $g(x, y, t)$ (Note: two-dimensional waves independent of z, the normal to the crystal surface)

$$g_{tt} - g_{xx} - g_{yy} + \mu^2[1 - 2/\cosh 2(\mu x)]g = 0 \quad (6)$$

and skyrmion emission (chiral instability) from within a domain wall in a direction x normal to the wall; skyrmions are created as a superposition of a deformation and a topological wave:

$$\begin{aligned} w = \exp\{-\mu[x &- (B/2)\tanh(\mu y + \mu t - \mu A) - \tanh(\mu y - \mu t + \mu A)] \\ &\times x \exp((i\pi/2)[\tanh(\mu y + \mu t - \mu A - \mu D) \\ &+ \tanh(\mu y - \mu t + \mu A + \mu D) + 2)]\}. \end{aligned} \quad (7)$$

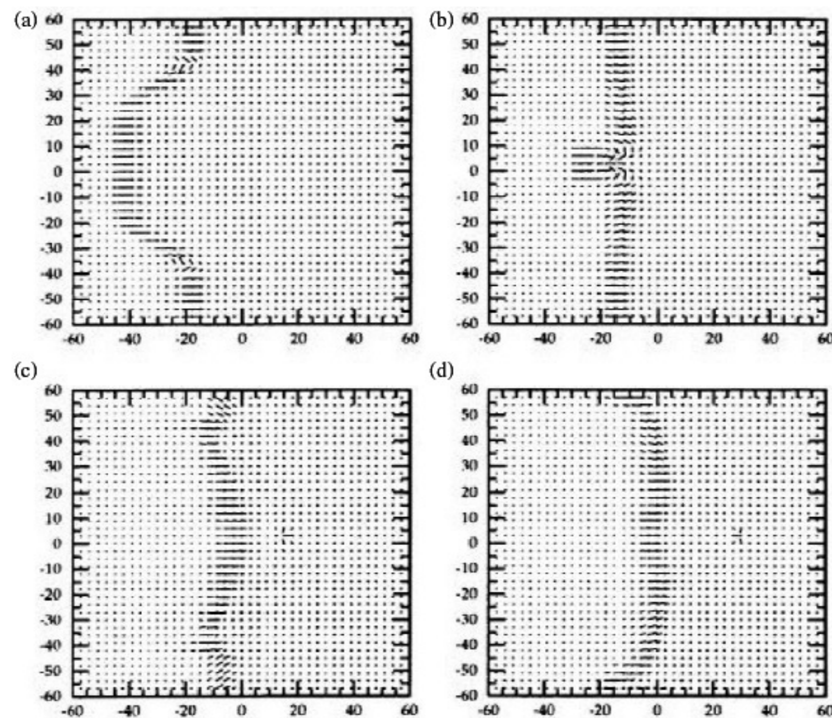

Figure 13. Calculations of nanodomains being ejected from inside a domain wall (Kudryavtsev *et al* 1998).

The time sequence shown in figure 13 is that for $A = 30$, $B = 20$, and $D = 10$ in equation (7), and corresponds reasonably well to data in figure 11, which occurs after the bulges develop. The nanodomain moves away from the larger wall at a speed which is half that of ripples along the wall, a prediction suitable for future testing in lead germanate. The theoretical model is more similar to the experimental data shown for iron garnet in figure 12. These comparisons suggest that the nanodomains in lead germanate (figure 11) do not nucleate at a distance from the large domain wall governed by depolarization fields, but rather originate within the wall and are ejected. If this is the case, it represents a completely new kind of nucleation in ferroelectrics: ferroelectric nucleation is almost always viewed as inhomogeneous, with only a few exceptions, on defect sites or interfaces; in the present situation it is inhomogeneous but nonlinear, arising at a threshold velocity, and in the complete absence of defects. This is further supported by a graph of number of nanodomains versus distance to the wall of the advancing large domain. If these nanodomains nucleated at a fixed distance from the wall, this graph should exhibit a peak; whereas if the domains are ejected from within the wall, the graph should be monotonically decreasing.

Perhaps the most important recent observation (Dawber *et al* 2006) is originally from Gruverman (1989) and is the fact that the nanodomains in lead germanate at high fields nucleate in completely different spots each time (figure 14). This is the opposite of the phenomena observed in all other ferroelectrics studied, where nucleation is inhomogeneous at defect sites (including electrode interfaces), as demonstrated by studies with pulsed laser photography synchronized to pulsed electric field application; in those cases the fact that nucleation always occurs at the same spot permits slow-motion movies of the nucleation and growth process by

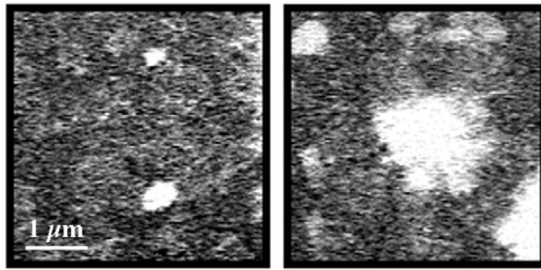

Figure 14. Atomic force microscopy of nucleation at random, irreproducible sites for successive voltage pulses in lead germanate (Dawber *et al* 2006).

varying the time delay between pulsed field E and nitrogen-laser flash. But for the nanodomains in lead germanate under higher fields, the spatial locations of nucleation are random and irreproducible, strongly supporting the skyrmion model.

The idea that domain walls are not flat has considerable support from studies by Paruch *et al* (2005), who measure a typical Hausdorf dimension of 2.5 rather than 2. Some authors have suggested, more generally, that ferroelectrics are a universality class having $d = 2.5$.

5.4. Ionic space-charge-limited current transients

The last decade has spawned much debate, sometimes acrimonious, about the nature of leakage currents in ferroelectric thin films. Generally speaking, there is evidence in different materials under different conditions of temperature and voltage (field) for space-charge-limited currents (SCLCs), for Poole–Frenkel bulk-limited conduction, and for Schottky (interface-limited) conduction. Many devices have a combination of two or three of these. There has also been some conjecture about Fowler–Nordheim tunnelling, but generally those inferences were made from rather narrowly restricted data over a small range of fields; Fowler–Nordheim conduction is now viewed as unlikely in these materials. These steady state studies will not be reviewed here, as they are peripheral to the nanoscale aspects of the material. We mention only a recent paper (Morrison *et al* 2005) that shows that such nanocrystals of barium titanate will withstand $E > 1$ GV m^{-1} and that at such fields the conduction mechanism is SCLC and not the variable-range hopping (Shlovskii 1973) inferred elsewhere (Fuchs *et al* 2001). However, the transient currents are specific to nanothicknesses in ferroelectric films.

5.4.1. Space-charge-limited transients. Independently Many and Rakavy (1962) and Mark and Helfrich (1962) developed a model of space-charge-limited current transients that exhibit cusps at a time t_p given by

$$t_p = \frac{0.78d^2}{\mu(T)V} \tag{8}$$

where μ is ionic carrier mobility and V, applied voltage. Zafar *et al* (1998a) fitted data to this model with success and determined the mobility, assumed to be from oxygen vacancies, as 2×10^{-12} cm^2 V^{-1} s^{-1}. Earlier Hofstein (1967) confirmed this model for oxide layers on Si. However, there are other time-dependent processes that must also be considered for such peaks in leakage current $I(t)$.

5.4.2. Cox–Tredgold mechanism. Cox and Tredgold (1965) found an electrolytic reaction for Au-electroded strontium titanate subjected to dc voltages. They attributed this to an

electrochemical process that spread out radially from their point contacts and hence gave a t^2 dependence of both affected area and resulting current. It generally resulted in a saturated plateau but under some circumstances was reversible.

5.4.3. Oxygen vacancy redistribution. Similar saturated plateaus were observed in $SrTiO_3$ ceramics and single crystals by Waser (Waser *et al* 1990a, 1990b, Baiatu *et al* 1990). The slow increase in conductivity was modelled in detail by an oxygen migration and accumulation process which results in a field enhancement at the cathode assumed to be blocking to oxygen ions. Oxygen vacancy redistribution and self-ordering was also reported to be responsible for fatigue in ferroelectric thin films (Dawber and Scott 2000, Scott and Dawber 2000). During charge and discharge measurements in BST films, Boikov *et al* (2002) identified current peaks which they suggested might also be due to oxygen vacancy migration.

5.4.4. Meyer's model. Recent numerical time-dependent simulations by Meyer *et al* (2005) showed how such peaks can arise not from true ionic conduction but instead due to oxygen vacancy migration and redistribution, which causes a modulation in the electronic conductivity and offers another possible explanation for Zafar's experimental findings.

Recently such high-field transient current peaks have been observed in 660 nm $SrTiO_3$ FIB-cut single-crystal $10 \times 10\ \mu m^2$ lamellae with gold electrodes by Zubko and Jung (2006), figure 15. The small electrode area allows fields of several MV cm^{-1} to be applied without breakdown, but also has the adverse effect of lowering the signal-to-noise ratio. Interpretation of these peaks awaits additional experimental data as well as further development of Meyer's model to include quantitative predictions for the voltage and temperature dependences.

6. Conduction mechanisms

In general the leakage current in ferroelectric films of nanometre thickness depends in a highly nonlinear way upon the thickness d. Several early attempts were made to combine Schottky, Poole–Frenkel, Fowler–Nordheim, and space-charge-limited mechanisms in pairs (Geppert 1962, Adirovich 1960a, 1960b, Stoeckmann 1963). Unfortunately these conductivities are not additive; instead a nonlinear integral equation generally results. This produces resistivities in oxide films that drop up to 12 orders of magnitude as the voltage is increased from zero to 5 V (Simmons 1971a, 1971b, Frank and Simmons 1967).

6.1. Schottky and Simmons

Although the more general thermionic emission–diffusion theory of Bethe is rarely mentioned, leakage data are often interpreted using its various special cases (see Baniecki *et al* 2003, Sze 1981) such as the 'standard Schottky equation' and the 'modified Schottky equation' due to Simmons (1965, 1971a, 1971b). When the mobility is high and transport is limited by the recombination velocity at the potential energy barrier maximum, Bethe's equation reduces to the standard Schottky expression. In cases of low mobility, Bethe's equation simplifies to that of Simmons and it is this variant which is more applicable to ferroelectrics as suggested by Scott (2000a) and shown experimentally by Zafar *et al* (1998b). Whilst Schottky conduction is clearly an interface-limited process, Simmons' equation (as pointed out by Zafar) involves both the carrier density at the potential barrier maximum near the interface *and* the mobility, which is a bulk property.

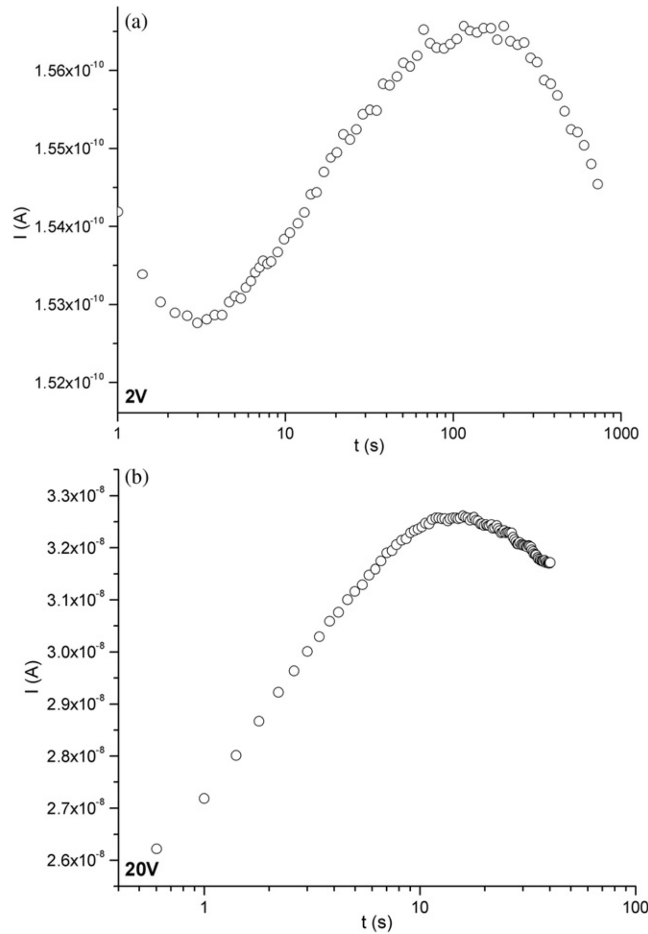

Figure 15. Transient current in 660 nm thick single-crystal strontium titanate sample provided by Dr J M Gregg (Queen's University, Belfast): $I(t)$ versus t, showing peak at approximately (a) 100 s at 2 V and (b) 10 s at 20 V (Zubko and Jung 2006).

It is important to note that in Simmons' equation

$$J(T, E) = \alpha T^{3/2} E\mu(m^*/m_0)^{3/2} \exp(-\phi_b/kT) \exp(\beta\sqrt{E}) \tag{9}$$

(here $\alpha = 3 \times 10^{-4}$ A s cm^{-3} K$^{-3/2}$; $\beta = (e/kT)(e/4\pi\varepsilon\varepsilon_0)^{1/2}$; μ is the mobility, m^* and m_0 are the effective carrier and free-electron masses respectively; ϕ_b—the zero field barrier height; and E, the field near the barrier maximum) there is an 'extra' factor of E (compared with the usual Schottky equation). For small E, this factor dominates the one in the exponent, and hence $J(E)$ will be proportional to E. This 'ohmic' dependence is, however, misleading, because Ohm's law requires two things: J proportional to V; and I inversely proportional to thickness d. The field E entering Schottky's and Simmons' expressions is, however, not necessarily linear in V as would be the case at high fields in the often assumed case of full depletion. In fact, recently the long-standing debate about the extent of depletion in ferroelectric thin films has resurfaced with the publication of a detailed self-consistent study by Pintilie and Alexe (2005) and Pintilie *et al* (2005) of PZT films analysed using a standard partial depletion model for semiconductors, modified to include the effects of ferroelectric polarization. This

conclusion of partial depletion supports the earlier model of Scott (1999) and is contrary to the inferences of Waser and co-workers or Hwang; however, we note that the specimens studied by Pintilie and co-workers were rather conductive (leaky), and thus their conclusions may have limited applicability. Even for high-resistivity Samsung PZT films, Delimova *et al* (2005) infer fully depleted Schottky conduction whereas Zubko and Jung (2006) infer Poole–Frenkel mechanisms. Scott (1999) has also given a careful explanation of why ε (in β) in equation (9) is the high-frequency dielectric constant $\varepsilon_\infty = N^2$, where N is the index of refraction, and is $5 < \varepsilon_\infty < 6$ rather than the dc dielectric constant $\varepsilon(0)$ of 300–1300.

6.2. Poole–Frenkel mechanism

Poole–Frenkel is a bulk-limited conduction mechanism that consists of field-assisted hopping from one defect site to another. In ferroelectrics such as barium titanate or PZT it involves Ti^{3+} sites (produced to ensure charge neutrality with respect to nearby oxygen vacancies). Poole–Frenkel conduction has the same $\exp E^{1/2}$ dependence as does Schottky (equation (9)). Although its prefactor differs by $4\times$ from that in the Schottky equation, this difference is not usually an unambiguous discriminator between the two mechanisms. This is usually expressed in terms of the fitted dielectric constant ε in equation (9); the factor of 2 difference in ε for the two mechanisms was clearly observed by Li and Lu (1991). As Kao and Hwang (1981) emphasize, experimental fittings of ε from such equations rarely give the correct independently known value, and in fact ε often varies for different voltage regimes. In the case of uniformly doped films Poole–Frenkel is most readily discriminated from Schottky current by varying the film thickness d, or by using different electrodes, both of which distinguish between bulk and interface-limited processes. However, when large impurity gradients are present the current may be limited by a particular region of the film and one may not expect to observe the linear scaling with thickness as is usual for bulk mechanisms.

6.3. Fowler–Nordheim tunnelling

Fowler–Nordheim tunnelling as a primary conduction mechanism has occasionally been suggested (Stolichnov and Tagantsev 1998, Stolichnov *et al* 1998, 1999, Baniecki *et al* 2001). However, in each case the fitting was done over a very limited range of fields E and temperatures. Extension to wider E values and lower T generally showed that tunnelling was not likely. In addition, the fitted tunnelling masses did not agree well with the known effective masses m^*. Although tunnelling masses and effective (band) masses need not in principle be the same, they are under conditions of tunnelling widths >2 nm (Conley and Mahan 1967) and typically match in careful experiments (Schnupp 1967).

6.4. Breakdown

Breakdown mechanisms in submicron films have been studied chemically (Lou *et al* 2006) and physically (Scott 2000a). Dendrite-like electrical shorts generally occur, which in PZT involve phase separation into lead oxide and rutile and in bismuth titanate result in Bi and O loss and pyrochlore production. The physical process is typically two-step, with electronic initiation followed by thermal run-away. This resembles avalanche and may be characterized in most cases as 'dc breakdown' rather than 'impulse breakdown', meaning that it is relatively independent of the voltage ramp rate $\mathrm{d}V/\mathrm{d}t$ applied (O'Dwyer 1964). The dependence of breakdown field upon thickness follows the law $E_\mathrm{B} = g(T)d^{-n}$ with $n = 0.3$–0.5 down to $d =$ about 30 nm.

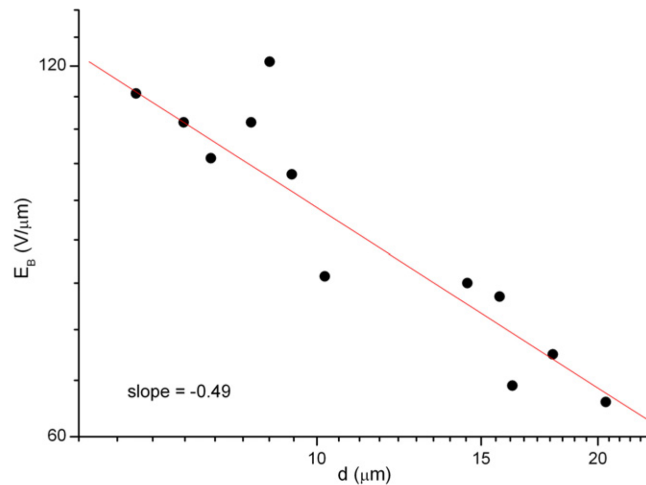

Figure 16. Breakdown field versus electrode separation d in $BaTiO_3$-based multilayer capacitors; data are for 4100 individual Ni base-metal electroded ceramic capacitors from 6 to 21 μm electrode separation d and 100–1500 μm^2 lateral electrode area. Below 6 μm (not shown) the breakdown field (for 61 000 samples) decreases with decreasing thickness (due to surface roughness); data from AVX Corp. (Milliken *et al* 2006).

6.4.1. Breakdown in multilayer capacitors. There is a large market for multilayer capacitors (thousands of millions per year) made of thin-film ferroelectric oxides. The breakdown field in this case also varies as $d^{-1/2}$, where d is here not the overall film thickness but rather the separation of electrodes within a stacked geometry. This is shown in figure 16 (Milliken *et al* 2006). Milliken's new work shows that the theory of thickness dependence of breakdown fields can be readily extended from single-layer capacitors to multilayer capacitors (MLCs) of thicknesses down to about 600 nm.

7. Tunnel junctions

Tunnel junctions have been fabricated from PZT films on strontium titanate substrates with strontium ruthenate electrodes (Contreras *et al* 2003a, 2003b). They have also been made with polyvinylidene difluoride (PVDF) (Qu *et al* 2003). For PZT areas of 2–200 μm^2 are produced by Ar ion-milling. The film thickness is typically 8–10 nm. Resistive switching is observed. The conduction mechanism is inferred to be variable-range hopping (Moran *et al* 2003); note that this is in contrast with the conduction results on 60–80 nm thick barium titanate (Morrison *et al* 2005) but compatible with the strontium titanate results reported by Fuchs *et al* (2001).

The mechanisms for the switching, and in particular the relationship between polarization switching at a coercive field E_c and resistive switching at a similar field threshold, are still not unambiguously sorted out (Kohlstedt *et al* 2002, Contreras 2003, Contreras *et al* 2003c, Bune *et al* 1995). This author's opinion is that the resistive switching is probably not related to tunnelling but is instead analogous to the ferroelectric Schottky diode reported earlier by Blom *et al* (1994). Resistive switching observed by Blom and co-workers is in 200 nm films; that by Dawber (2005) is in 20 nm films (large changes of 300 000%, from 2 to 6 kΩ with polarity reversal!). But in either case these thicknesses are too great for any direct tunnelling (which requires thickness <6 nm or so, according to Simmons or Frank and Simmons). Therefore the direct tunnelling models seem unrealistic.

8. Polyvinylidene difluoride (PVDF)

There have been a series of papers by Bune, Fridkin, Ducharme and co-workers which claim (Bune *et al* 1998, Ducharme *et al* 2000, Ducharme and Fridkin 2002a, 2002b) that Langmuir–Blodgett films of PVDF are two-dimensional ferroelectrics and/or that they switch without any domain wall motion. It has been known since the inception of Landau theory that ferroelectrics indeed could conceivably switch with every ion reversing local polarization simultaneously, and thus going from a single up-domain to a single down-domain with no domain wall motion. However, the coercive field required for this domain-free process is estimated as $>1000\times$ the normal coercive field for domain-dominated processes. Aside from the initial authors' claims, no support has been found for this hypothesis for PVDF switching; other interpretations of their data have been given by Bratkovsky and Levanyuk (2000), by Scott (2000a, 2000b, 2003), by Moreira (2002) and by Kliem and Tadros-Morgane (2005). The latter authors refer to the domain-motion switching process as 'extrinsic' and the simultaneous reversal of all polarizations without domain wall motion as 'intrinsic', labels we do not advocate.

9. Circular and toroidal ordering

Over the past 60 years several physicists have considered the possibility that magnetic spins or electric polarization vectors might order not rectilinearly—parallel and/or antiparallel—but in circles or toroids. Kittel (1946) was the first to show that this was likely for ferromagnets as their size decreased to nanodots; the extension to ferroelectrics was made around 1984 by Ginzburg *et al* (1984) and by Sannikov (1985), Sannikov and Zheludev (1985), Sannikov (1998) with a follow-up a decade later by Gorbatsevich and Kopaev (1994). This work lay largely unnoticed, despite its emphasis in excellent reviews by Schmid (1994, 2001), until it was resurrected and put on an *ab initio* basis by Naumov *et al* (2004) and also discussed by Scott (2005). The basic idea is illustrated in figure 17, and the argument is that such structures are NOT the minimum free-energy state except for very small objects (nanodots or nanowires) and at low temperatures. It is important to note that there are two unrelated causes of circular or toroidal ferroelectricity: in nanodots 90° domains can produce circular ordering due to the surface boundary conditions (Kittel 1946). This requires no magnetoelectric coupling between polarizations and spins. But in bulk circular or toroidal ordering can arise in multiferroics due to magnetoelectric coupling. The same terminology is recently in use for both cases, but the physics is rather unrelated.

The search for such structures initially met the same fate as did the notorious examples of cold fusion or poly-water: first it was reported (Zheludev *et al* 1974) but then never reproduced, so that a black cloud lay over the topic for many years. At present several groups are looking carefully via electron microscopy and AFM (atomic force microscopy) in ferroelectric nanostructures for such domains, and a detailed model, including switching mechanisms, has been proposed (Ponomareva *et al* 2005a, 2005b, Prosandeev *et al* 2006).

Fiebig (2006) has very recently reported that toroidal domains have already been observed, but initially misinterpreted, in $YMnO_3$. An excellent theoretical review on this topic is by Mermin (1979).

10. Magnetoelectrics (multiferroics)

Several good reviews have been published. The best of the early summaries is Schmid (1994). Very recent ones include Fiebig (2005) and Eerenstein *et al* (2006a). With regard to nanomaterials *per se* there have been particularly relevant issues concerning 'nano' properties:

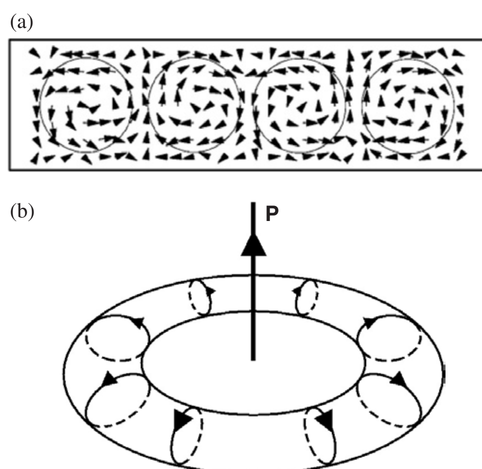

Figure 17. Schematic patterns of (a) circular (Naumov *et al* 2004) and (b) toroidal (Gorbatsevich and Kopaev 1994) polarizations in ferroelectrics.

firstly, in bismuth ferrite $BiFeO_3$, in bulk the spins have an incommensurate helical ordering that causes the magneto-electric effect to average spatially to near-zero. It was proposed (Wang *et al* 2003, 2005) that in thin-film form the boundary conditions unwind the helix (as in the surface-stabilized ferroelectric liquid crystals of Lagerwall and Clark (1980)), resulting in a large magnetization; but the reported magnetization of 1 μ_B/cell appears to be an artefact caused by mixed Fe valence (and possibly oxygen vacancies), as shown by Eerenstein *et al* (2005). $BiFeO_3$ in thin film apparently has a small magnetization of $<0.1\ \mu_B$/cell, and interest has diminished; although it still merits attention as a lead-free ferroelectric, its conductivity is usually too high for practical devices.

Bismuth manganite $BiMnO_3$ is also quite interesting. In nanothicknesses it has a phase change at a critical thickness of 70 ± 10 nm (Eerenstein *et al* 2006b) due to lattice-mismatch stress relaxation. Ferroelectricity in $BiMnO_3$ is still moot. Data suggest a linear lossy dielectric.

Many recent papers describe magneto-capacitance effects or 'magneto-dielectrics'. This is a change in dielectric constant with applied magnetic field. Unfortunately such changes, which can be very large—450% in spinel (Hemberger *et al* 2005)—or 10 000% in other materials (Egami 2006), may often be due to artefacts: Maxwell–Wagner relaxation in a magnetoresistive material (Catalan 2006); no magnetoelectric coupling is required, and the effect is probably useless for devices.

The early work on magnetoelectrics was entirely on bulk materials and started with Cr_2O_3 around 1960 (Dzyaloshinskii 1957, Astrov 1960) and then emphasized boracites through the 1970s (Ascher *et al* 1966). The renaissance since 1995 has been on manganites and especially Tb compounds (Hur *et al* 2004, Saito and Kohn 1995, Kimura *et al* 2003) and has extended research into very thin films. The search for a material that is both ferroelectric and a strong ferromagnet (not a canted antiferromagnet) at room temperature is still unsuccessful. A commercial device would probably require very high electrical resistivity ($>10^6\ \Omega$ cm) as well; following the original line of work by Smolenskii in the 1970s, this is being pursued (Palkar *et al* 2004) by doping $BiFeO_3$ with other elements, both at the A-site (e.g., Pb) and the B-site.

Commercial multiferroic devices using magnetoelectric effects are apt to involve thin-film laminated bimorphs (Bai *et al* 2005) of strong magnetoelastics (e.g., terphenyl) and strong electrostrictive or piezoelectrics (e.g., PZT). These have a combined magnetoelectric

coupling (albeit indirect through strain) of order a thousand times greater than that in magnetoelectrics having direct coupling between polarization P and magnetization M. In the latter the magnetoelectric susceptibility χ^{me} is required to be $\leqslant \chi^{e}\chi^{m}$, the product of electric and magnetic susceptibilities; the indirect coupling through strain gives a coupling a thousand times stronger than this limit. Although the near-term application of magnetoelectrics to memory devices looks unpromising, their use as sensors generates more optimism, and the replacement of superconducting quantum interference devices (SQUIDs) by laminated multiferroic bimorphs (e.g., terphenyl-PZT) is quite likely, since the sensitivities are comparable and the SQUIDs cost more than a thousand times more (about \$1000 versus \$1).

11. The future

It is interesting perhaps to speculate about the next ten years in nanoferroelectrics: the main commercial application of ferroelectrics <150 nm thick and <500 nm in lateral width will be for (3D) DRAMs and FRAMs. On the pure science side, toroidal ordering will be studied, including switching. Electrical switching of magnetic materials (and vice versa) will be examined. Studies of nanoscale ferroelectrics at millikelvin temperatures will be carried out to look for more examples of quantum criticality and for confinement energies (ultra-thin single crystals of strontium titanate, which has remarkably high mobility at cryogenic temperatures, are a good choice for both). Nonlinear mechanisms of domain nucleation and growth (skyrmions) will be studied optically and electrically. Non-planar geometries of ferroelectric nanowires and nanotubes will be examined and used for microfluidic and microelectronic applications. Finally, devices which combine carbon nanotubes (conductors) and ferroelectric nanotubes (piezoelectric insulators) will generate complex electrical devices, including nanotransducers and nanoactuators. Self-assembly of such nanoarrays (Alexe *et al* 1998, Dawber *et al* 2003) will be emphasized.

Acknowledgment

Work supported by the EPSRC.

References

Adirovich E I 1960a *Fiz. Tverd. Tela* **2** 1410
Adirovich E I 1960b *Sov. Phys.—Solid State* **2** 1282 (Engl. Transl.)
Alexe M, Gruverman A, Hamagea C, Zakharov N D, Pignolet A, Hesse D and Scott J F 1999 *Appl. Phys. Lett.* **75** 1158
Alexe M, Scott J F, Curran C, Zakharov N D, Hesse D and Pignolet A 1998 *Appl. Phys. Lett.* **73** 1592
Andreev A F 1981 *JETP Lett.* **53** 1063
Ascher E, Rieder H, Schmid H and Stössel H 1966 *J. Appl. Phys.* **37** 1404
Astrov D N 1960 *Zh. Eksp. Teor. Fiz.* **38** 984
Auciello O 2006 *J. Appl. Phys.* at press
Bai F *et al* 2005 *Appl. Phys. Lett.* **86** 032511
Baiatu T, Waser R and Härdtl K-H 1990 *J. Am. Ceram. Soc.* **73** 1663
Baniecki J D *et al* 2001 *J. Appl. Phys.* **89** 2873
Baniecki J D *et al* 2003 *Mater. Res. Soc. Symp. Proc.* **748** 441
Batra I P, Wurfel P and Silverman B D 1973 *J. Vac. Technol.* **10** 687
Blom P W M, Wolf R M, Cillessen J F M and Krijn M P C M 1994 *Phys. Rev. Lett.* **73** 2107
Bobylev S V *et al* 2003 *J. Phys.: Condens. Matter* **15** 7925
Boikov Yu A, Goltsman B M, Yamarkin V K and Lemanov V V 2002 *Appl. Phys. Lett.* **80** 4003
Bratkovsky A M and Levanyuk A P 2000 *Phys. Rev. Lett.* **87** 019701
Bratkovsky A M and Levanyuk A P 2005 *Phys. Rev. Lett.* **94** 107601

Bune A V *et al* 1995 *Appl. Phys. Lett.* **67** 3975
Bune A V *et al* 1998 *Nature* **391** 874
Catalan G 2006 *Appl. Phys. Lett.* at press
Chandra P, Dawber M, Littlewood P B and Scott J F 2004 *Ferroelectrics* **313** 7
Cho Y *et al* 2002 *Appl. Phys. Lett.* **81** 4401
Conley J W and Mahan G D 1967 *Phys. Rev.* **161** 681
Contreras J R 2003 *PhD Thesis* Cologne
Contreras J R *et al* 2003a *Appl. Phys. Lett.* **83** 495
Contreras J R *et al* 2003b *Appl. Phys. Lett.* **83** 126
Contreras J R *et al* 2003c *MRS Proc.* **688** C8.10
Cox G A and Tredgold R H 1965 *Brit. J. Appl. Phys.* **16** 427
Dawber M 2005 private communication
Dawber M, Chandra P, Littlewood P B and Scott J F 2003 *J. Phys.: Condens. Matter* **15** L393
Dawber M, Gruverman A and Scott J F 2006 *J. Phys.: Condens. Matter* at press
Dawber M, Rabe K M and Scott J F 2005 *Rev. Mod. Phys.* **77** 1083
Dawber M and Scott J F 2000 *Appl. Phys. Lett.* **76** 1060
Dawber M, Szafraniak I, Alexe M and Scott J F 2003 *J. Phys.: Condens. Matter* **15** L667
Delimova L A *et al* 2005 *Appl. Phys. Lett.* **87** 192101
Du X-F and Chen I-W 1997 *Appl. Phys. Lett.* **72** 1923
Du X-F and Chen I-W 1998 *Appl. Phys. Lett.* **75** 4186
Ducharme S *et al* 2000 *Phys. Rev. Lett.* **84** 175
Ducharme S and Fridkin V M 2002a *Phys. Rev. Lett.* **87** 019701
Ducharme S and Fridkin V M 2002b *Phys. Rev. Lett.* **88** 179701
Dzyaloshinskii I E 1957 *Zh. Eksp. Teor. Fiz.* **33** 807
Eerenstein W, Mathur N D and Scott J F 2006a *Nature* at press
Eerenstein W, Morrison F D, Dho J H, Blamire M G, Scott J F and Mathur N D 2005 *Science* **419** 1203a
Eerenstein W, Morrison F D, Scott J F and Mathur N D 2006b at press
Egami T 2006 *Workshop on Fundamentals of Ferroelectrics (Williamsburg, VA, Feb.)*
Fiebig M 2005 *J. Phys. D: Appl. Phys.* **38** R1
Fiebig M 2006 *Annual Meeting German Physical Society and European Physical Society (Dresden, March 2006)*
Frank G and Simmons J G 1967 *J. Appl. Phys.* **38** 832
Fridkin V M 2002 private communication
Fuchs D, Adam M and Schneider R 2001 *J. Physique* IV **11** 71
Fujisawa H, Okaniwa M, Nonomura H, Shimizu M and Niu H 2004 *J. Eur. Ceram. Soc.* **24** 641
Funakubo H *et al* 2005 *Mater. Sci. Eng.* B **120** at press
Ganpule C S *et al* 1999 *Appl. Phys. Lett.* **75** 409
Geppert D V 1962 *J. Appl. Phys.* **33** 2993
Ginzburg V L, Gorbatsevich A A, Kopaev Yu V and Volkov B A 1984 *Solid State Commun.* **50** 339
Glinchuk M D, Eliseev E A and Stephanovich V A 2002 *Physica* B **322** 356
Gorbatsevich A A and Kopaev Yu V 1994 *Ferroelectrics* **161** 321
Goux L *et al* 2005 A highly reliable three-dimensional integrated SBT ferroelectric capacitor enabling FeRAM scaling *IEEE Trans.* **52** 447
Gregg J M *et al* 2006 at press
Gruverman A 1989 *PhD Thesis* Ural State University, Ekaterinburg, Russia
Guro G M *et al* 1968 *Sov. Phys.—Solid State* **10** 100
Guro G M *et al* 1970 *Sov. Phys.—Solid State* **11** 1574
Gutkin M Yu *et al* 2000 *J. Phys.: Condens. Matter* **12** 5391
Gutkin M Yu *et al* 2001 *Phys. Status Solidi* **184** 485
Hartmann A J *et al* 1999 *Integr. Ferroelectr.* **23** 113
Hemberger J *et al* 2005 *Nature* **434** 364
Hofstein R 1967 *Appl. Phys. Lett.* **10** 291
Hur N, Park S, Sharma P A, Ahn J S, Guha S and Cheong S-W 2004 *Nature* **429** 92
Ishibashi Y and Takagi Y 1971 *J. Phys. Soc. Japan* **31** 506
Ishiwara H, Okuyama M and Arimoto Y 2004 *Ferroelectric Random Access Memories* (Heidelberg: Springer)
Ivanchik I I 1961 *Fiz. Tverd. Tela* **3** 3731
Jung D J, Dawber M and Scott J F 2002 *Integr. Ferroelectr.* **48** 59
Jung D J, Kim K and Scott J F 2005 *J. Phys.: Condens. Matter* **17** 4843
Junquera J and Ghosez P 2003 *Nature* **422** 506

Kao K C and Hwang W 1981 *Electrical Transport in Solids* (Oxford: Pergamon) p 315
Kay H F and Dunn J W 1962 *Phil. Mag.* **7** 2027
Kenis P J A and Stroock A D 2006 *MRS Bull.* **31** 87
Kimura T, Goto T, Shintani H, Ishizaka K, Arima T and Tokura Y 2003 *Nature* **426** 55
Kittel C 1946 *Phys. Rev.* **70** 965
Kliem H and Tadros-Morgane R 2005 *J. Phys. D: Appl. Phys.* **38** 1860
Kohiki S, Takada S, Shimizu A, Yamada Y and Mitone M 2000 *J. Appl. Phys.* **87** 474
Kohlstedt H, Pertsev N A and Waser R 2002 *MRS Proc.* **688** C.6.5
Kretschmer R and Binder K 1979 *Phys. Rev.* B **20** 1065
Kudryavtsev A, Piette B M A G and Zakrzewski W J 1998 *Nonlinearity* **11** 783
Lagerwall S T and Clark N A 1980 *Appl. Phys. Lett.* **36** 899
Landauer R, Young D R and Drougard M E 1956 *J. Appl. Phys.* **27** 752
Li J, Nagaraj B, Liang H, Cao W, Lee H and Ramesh R 2004 *Appl. Phys. Lett.* **84** 1174
Li P and Lu T-M 1991 *Phys. Rev.* B **43** 14261
Li S, Eastman J A, Newnham R E and Cross L E 1996 *Japan. J. Appl. Phys.* **35** L502
Li S *et al* 1997 *Japan. J. Appl. Phys.* **36** 5169
Lou X, Hu X, Zhang M, Morrison F D, Redfern S A T and Scott J F 2006 *J. Appl. Phys.* **99** 044101
Ma D, Harnagea C, Hesse D and Goesele U 2003 *Appl. Phys. Lett.* **83** 3770
Ma W and Hesse D 2004 *Appl. Phys. Lett.* **84** 2871
Many A and Rakavy G 1962 *Phys. Rev.* **126** 1980
Mark P and Helfrich H W 1962 *J. Appl. Phys.* **33** 205S
Menou N *et al* 2005 *Appl. Phys. Lett.* **87** 073502
Mermin N D 1979 *Rev. Mod. Phys.* **51** 591
Meyer R, Liedtke R and Waser R 2005 *Appl. Phys. Lett.* **86** 112904
Milliken A D, Bell A J and Scott J F 2006 Scaling of breakdown field with inter-electrode separation in multi-layer capacitors *Appl. Phys. Lett.* submitted
Mitsui T and Furuichi J 1953 *Phys. Rev.* **90** 193
Miyake M, Scott J F, Morrison F D, Tatsuta T and Tsuji O 2006 *Integr. Ferroelectr.* at press
Moran O, Hott R, Schneider R and Halbritter J 2003 *J. Appl. Phys.* **94** 6717
Moreira R L 2002 *Phys. Rev. Lett.* **88** 179701
Morrison F D, Ramsay L and Scott J F 2003 *J. Phys.: Condens. Matter* **15** L527
Morrison F D *et al* 2005 *Appl. Phys. Lett.* **86** 152903
Nagarajan V *et al* 2004 *Appl. Phys. Lett.* **84** 5225
Naumov I, Bellaiche L and Fu H 2004 *Nature* **432** 737
Nonomura H, Fujisawa H, Shimizu M, Niu H and Honda K 2003 *Japan. J. Appl. Phys.* **42** 5918
O'Dwyer J J 1964 *Theory of Dielectric Breakdown in Solids* (Oxford: Clarendon)
Palkar V R, Ganesh Kumara K and Malik S K 2004 *Appl. Phys. Lett.* **84** 2856
Paruch P, Giamarchi T and Triscone J-M 2005 *Phys. Rev. Lett.* **94** 197601
Pintilie L and Alexe M 2005 *J. Appl. Phys.* **98** 124103
Pintilie L *et al* 2005 *J. Appl. Phys.* **98** 124104
Ponomareva I, Naumov I and Bellaiche L 2005a *Phys. Rev.* B **72** 214118
Ponomareva I, Naumov I, Kornyev I, Fu H and Bellaiche L 2005b *Phys. Rev.* B **72** 140102
Prasertchoung S *et al* 2004 *Appl. Phys. Lett.* **84** 3130
Prosandeev S *et al* 2006 *Integr. Ferroelectr.* at press
Pulvari C and Kuebler W 1958 *J. Appl. Phys.* **29** 1742
Qu H *et al* 2003 *Appl. Phys. Lett.* **82** 4322
Randoshkin V V 1995a *Fiz. Tverd. Tela* **37** 356
Randoshkin V V 1995b *Sov. Phys.—Solid State* **37** 355 (Engl. Transl.)
Rice T M, Whitehouse S and Littlewood P B 1981 *Phys. Rev.* B **24** 2751
Roelofs A, Schneller T, Szot K and Waser R 2002 *Appl. Phys. Lett.* **81** 5231
Roytburd A 1976 *Phys. Status Solidi* a **37** 329
Saad M, Baxter P, Bowman R M, Gregg J M, Morrison F D and Scott J F 2004 *J. Phys.: Condens. Matter* **16** L451
Saito K and Kohn K 1995 *J. Phys.: Condens. Matter* **7** 2855
Sannikov D G 1985 *JETP Lett.* **41** 277
Sannikov D G 1998 *Ferroelectrics* **219** 177
Sannikov D G and Zheludev I S 1985 *Sov. Phys.—Solid State* **27** 826
Schilling A *et al* 2006 at press
Schmid H 1994 *Ferroelectrics* **161** 1

Schmid H 2001 *Ferroelectrics* **252** 41
Schnupp P 1967 *Phys. Status Solidi* **21** 567
Scott J F 1999 *Ferroelectrics* **232** 25
Scott J F 2000a *Ferroelectric Memories* (Heidelberg: Springer) p 132
Scott J F 2000b *J. Appl. Phys.* **88** 6092
Scott J F 2003 *Ferroelectrics* **291** 205
Scott J F 2005 *Nat. Mater.* **4** 13
Scott J F, Alexe M, Zakharov N D, Pignolet A, Curran C and Hesse D 1998 *Integr. Ferroelectr.* **21** 1
Scott J F and Dawber M 2000 *Appl. Phys. Lett.* **76** 3801
Scott J F, Godfrey R B, Araujo C A, McMillan L D, Meadows H B and Golabi M 1986 *ISAF: Proc. 6th IEEE Int. Symp. Appl. Ferroelec.* ed W Smith (Piscataway, NJ: IEEE) p 569
Shchukin V A and Bimberg D 1999 *Rev. Mod. Phys.* **71** 1125
Shimizu M, Okaniwa M, Fujisawa H and Niu H 2004 *J. Eur. Ceram. Soc.* **24** 1625
Shlovskii B I 1973 *Sov. Phys.—Semicond.* **6** 1964
Shur V Ya, Gruverman A, Ponomarev N Yu, Rumyantsev E L and Tonkacheva N A 1990 *Ferroelectrics* **111** 197
Shur V Ya, Gruverman A, Ponomarev N Yu, Rumyantsev E L and Tonkacheva N A 1991 *JETP Lett.* **53** 615
Siefert A, Vojta A, Speck J S and Lange F F 1996 *J. Mater. Res.* **11** 1470
Simmons J G 1965 *Phys. Rev. Lett.* **15** 967
Simmons J G 1971a *J. Phys. Chem. Solids* **32** 1987
Simmons J G 1971b *J. Phys. Chem. Solids* **32** 2581
Stoeckmann F 1963 *Phys. Status Solidi* **3** 221
Stolichnov I and Tagantsev A K 1998 *J. Appl. Phys.* **84** 3216
Stolichnov I, Tagantsev A K, Colla E L and Setter N 1998 *Appl. Phys. Lett.* **73** 1361
Stolichnov I, Tagantsev A K, Colla E L and Setter N 1999 *Ferroelectrics* **225** 125
Streiffer S K *et al* 2002 *Phys. Rev. Lett.* **89** 067601
Sze S M 1981 *Physics of Semiconductor Devices* (New York: Wiley) section 5.4
Tagantsev A K, Stolichnov I, Setter N, Cross J S and Tsukada M 2002 *Phys. Rev.* B **66** 214109
Tilley D R and Zeks B 1984 *Solid State Commun.* **49** 823
Tybell T, Ahn C H and Triscone J-M 1999 *Appl. Phys. Lett.* **75** 856
Tybell T, Paruch P, Giamarchi T and Triscone J-M 2002 *Phys. Rev. Lett.* **89** 097601
Vul B M *et al* 1970 *Sov. Phys.—Semicond.* **4** 128
Wang J *et al* 2003 *Science* **299** 1719
Wang J *et al* 2005 *Science* **419** 1203b
Waser R, Baiatu T and Härdtl K-H 1990a *J. Am. Ceram. Soc.* **73** 1645
Waser R, Baiatu T and Härdtl K-H 1990b *J. Am. Ceram. Soc.* **73** 1654
Watts B E, Leccabue F, Tallarida G, Ferrari S, Fanciulli M and Padeletti G 2004 *Integr. Ferroelectr.* **62** 3
Williams R S, Medeiros-Ribeiro G, Kamins T I and Oldberg D A A 2000 *Annu. Rev. Phys. Chem.* **51** 527
Wouters D 2006 *Int. Symp. Integ. Ferroelec. (Shanghai, 2005): Integr. Ferroelectr.* at press
Wu X, Vanderbilt D and Hamann D R 2005 *Phys. Rev.* B **72** 035105
Yacoby Y 2006 *Workshop on Fundamentals of Ferroelectricity (Williamsburg, VA, Feb.)*
Yanase N, Abe K, Fukushima N and Kawakubo T 1999 *Japan. J. Appl. Phys.* **38** 5305
Yoon J-G *et al* 2006 *Workshop on Fundamentals of Ferroelectricity (Williamsburg, VA, Feb.)*
Yu B, Zhu C and Gan F 1997 *J. Appl. Phys.* **82** 4532
Zafar S *et al* 1998a *Appl. Phys. Lett.* **73** 175
Zafar S *et al* 1998b *Appl. Phys. Lett.* **73** 3533
Zhang J, Zhen Y, Zhang M-S and Scott J F 2001 *Solid State Commun.* **118** 241
Zheludev I S, Perekalina T M, Smirnovskaya E M, Fonton S S and Yarmukhamedov Yu N 1974 *JETP Lett.* **20** 129
Zhirnov V A 1958 *J. Eksp. Teor. Fiz.* **35** 1175
Zhirnov V A 1959 *Sov. Phys.—JETP* **35** 822 (Engl. Transl.)
Zhou W *et al* 1992 *J. Solid State Chem.* **101** 1
Zubko P and Jung D-J 2006 unpublished